Proceedings of ASME PVP Division Conference:
5th International Symposium on
Computational Technologies for Fluid/Thermal/Chemical/
Stressed Systems with Industrial Applications
July 25-29, 2004, San Diego/La Jolla, USA

HEMODYNAMIC PRESSURE INSTABILITIES AND THEIR RELATION TO HEART AUSCULTATION

Vladimir Kudriavtsev
Biosignetics Corporation, Toronto
Ontario, M2H3M3 CANADA
info@bsignetics.com

Vladimir Polyshchuk
Biosignetics Corporation, Exeter
New Hampshire 87544
info@bsignetics.com

Olga Saynina
Biosignetics Corporation, Toronto
Ontario, M2H3M3 CANADA

ABSTRACT

We present work in progress results showing how CFD can be utilized to study heart sound acoustic signatures. Special emphasize is given to the dynamics of cardiac cycle, its fluid mechanics interpretation and to the structure of the heart sounds S1 and S2.

INTRODUCTION

Sound based heart diagnostic is called auscultation and is performed by the physician using the stethoscope or some digital recording device (see Fig. 1). A visual representation of the heart sound amplitude time plot is called a phonocardiogram, or PCG (Figs. 2a, 4a). It is another tool that is frequently used by the physicians to assist in auscultation. The skill to detect and diagnose the heart problem by auscultation and phonocardiogram can take years to acquire and refine [1]. Human heart diagnostics using auscultation and PCG requires a proper understanding of the nature, causes and changes in these sounds. Understanding the cause of the heart sounds is a complex multidisciplinary problem. It will be demonstrated in this paper by analyzing normal heart sound pattern and its two basic components that are called S1(Fig. 2a) and S2 (Fig. 3a). These sounds are always present in the PCG of a normal healthy person (Fig.4a). Considerable amount of research was devoted to the synthesis of S1 and S2, but to this date their genesis is not fully understood [2,3,4]. It is recognized that both S1 and S2 consist of multiple components. Researchers usually distinguish up to four components in S1 sound [4]. Two of these components are labeled M1 and T1, for being a result of the mitral and tricuspid valve closures [5]. The S2 heart sound is recognized to have at least two components named A2 and P2. They were associated with work of the aortic and pulmonary heart valves [2,5]. Many medical textbooks on auscultation attribute the genesis of these sounds to “blood flow turbulence” or omit detailing the subject matter [6]. This paper will attempt to contribute to develop better understanding of the S1 and S2 sounds through the use of computational fluid dynamics.

NORMAL HEART SOUND STRUCTURE

We analyzed the structure of a normal heart sound using an experimentally obtained sound sample. Digital recording of a normal healthy person was made using the electronic stethoscope Cardionics E-Scope II, laptop with a sound card and Windows Sound Recorder (see Fig. 1). The sampling rate of the recorder was set to 44.1 kHz. The recorded sound was stored in wave file format and processed using commercially available software BSignal -Phonocardiograph [8]. Figures 2(a,b) and 3(a,b) demonstrate the individual heart sound components S1 and S2 and their corresponding FFT spectrums. A complete single beat segment of the heart sound and corresponding FFT spectrogram are shown in Figures 4(a,b).

Although the PCG charts of S1 and S2 (Figs. 2a, 3a) may appear somewhat similar, the comparison of their FFT spectrum clearly indicates that these signals are in fact structurally different. The S1 sound spectrum has a major

peak at 30 Hz, while S2 has two peaks at 41 Hz and 120 Hz. Thus, S1 produces soft or dull sound, while S2 produces higher pitched distinct sound. This confirms through the measurement an established fact that these signals do differ in their genesis [4]. Five peak components of S1 were sequentially numbered from 1 to 5 in Figure 2a and are named as $S1_1$,…,$S1_5$ for the future references. The second and third peaks in S1 are the strongest and are called M1 and T1 respectively. According to widely accepted Rushmer's theory [4,7] low amplitude first peak ($S1_1$) manifests the beginning of the S1. PCG timings are presented in Tables 1-3. S1 starts at 92ms and S2 sound begins at 158 ms. The S1 signal ends after its 5th peak at 225 ms. Thus, the S1 duration was estimated at 133 ms. In a similar manner, the duration of S2 was determined to be 80 ms. While Table 1 gives the time for the beginning and the end of these sounds, Tables 2 and 3 show detailed timing for each peak, and corresponding peak-to-peak durations. These durations are important characteristics of an individual heart.

The physical events occurring during the cardiac cycle can be directly related to the peaks in S1 and S2. A simplified visual representation of the heart operational dynamics (cardiac cycle) is given in Figure 5 and various important events (#1-14) are itemized on the table below the schematics. The right side of the heart consists of the atrium and ventricular chambers separated by a tricuspid valve T. Left side of the heart also consists of the left atrium and left ventricular chamber separated by the mitral valve M. Deoxygenated blood flows from the right ventricle through the pulmonary arteries into the lungs passing through the pulmonary valve P. Enriched in oxygen blood returns from the lungs through the pulmonary veins into the left atrium. From the left ventricle the blood is pushed through the aortic valve A into the arteries [5,6].

Figure 5 describes the timing of the events as they occur during the systolic period of a cardiac cycle and relates them to the mechanics of S1 sound. At the beginning of the cycle, both tricuspid and mitral valves (also called atrio-ventricular valves, or AV) are opened and blood freely flows into the left and right ventricles (events #1,2). The pulmonic and aortic valves are closed during this period. The backflow of the blood from the aortic valve causes the mitral valve to close first (event #2) and produces M1 (2nd) peak in S1. Shortly afterwards, the blood backflow from the pulmonic valve causes the closure of the tricuspid valve T (event #3). This event corresponds to the T1 (3rd) peak in S1. In case of the signal shown in Figure 2a, the time that passed between M1 and T1 was equal to 32 ms. A time gap between T1 and M1 is estimated in the literature to be between 20 to 30 ms [5]. Once all heart valves are closed (event #3), the isovolumic ventricular contraction of the left and right heart ventricles commences (event #4). The ventricles contract giving the rise to the pressure in the ventricles, they last approximately 20-30 ms. In S1 recorded in Fig. 2a, the time gap between 2nd and 3rd peaks is equal to 26ms. The pressure rise in the ventricles causes aortic valve to open first (#5) following by the opening of the pulmonic valve (event #6).

We will need to establish the correspondence between the cardiac cycle events and the signal peaks on S1 and S2. We assume that these signal peaks can be directly correlated with the pressure oscillations inside the heart chambers. These pressure oscillations are produced by the vibrating membranes of the closed heart valves. They are at their maximum amplitudes when heart chamber volumes are tightly closed, thus producing a resonant cavity with a standing wave. We assume that the sound waves can reflected from the walls and then dissipate in the heart chambers. Thus, we do not consider them in this paper. This contemplation will require coupled fluid flow and acoustic equations solution.

We simulate $S1_1$ peak as a result of an initial blood flow impact against the pulmonary and aortic valves. These closed valves work as a membrane, and resulting pressure wave generates first $S1_1$ peak and forces an immediate closure of the AV valves. Pressure wave is then reflected from AV valves (M, T). It travels back to the semilunar valves producing another pressure peak. This is also assisted by the isovolumic contraction of both ventricles. Subsequently, semilunar valves (P, A) do open and release the flow into the pulmonary and aortic cavities. We postulate that this flow discharge does not produce any major sound peaks and results in a pressure decrease inside the ventricles effectively causing S1 to end (see for example Fig. 9b). We postulate that in case of the normal valvular heart function there should be no additional pressure spikes associated with the flow discharge through the semilunar valves into the aortic and pulmonary areas. According to the literature [4,7], some researchers associate valve openings (P, A) with the last sound peaks in S1. Our initial assessment and CFD analysis do not support this theory. Nature had designed these valves to minimize associated flow transients, instabilities and pressure fluctuations. However, in case of a broken or improper valvular function, we may anticipate noticeable flow instabilities. Such instabilities (see for example Fig. 6 and 8a) can be related with what physicians call early, mid-systolic and late systolic **murmurs**. Murmurs typically have much higher frequencies (100-150 Hz), which can be explained with a smaller characteristic dimension of the respective flow cavities. For instance, 1 cm size volume with 1 m/s flow velocity generates 100 Hz characteristic frequency. For S1 peaks, characteristic frequency is related to the size of the ventricles and should be on the order of f = 120 [cm/s]/ 4 [cm] = 30 Hz. S2 is generated by the same aortic and pulmonary valves after they reach closed position. Sound generation process follows the same footsteps as for S1. Flow passes through the valves and

reaches an opposite side of the aorta and pulmonary cavities. These cavities has smaller characteristic flow dimension than the ventricles. Thus, we estimate that characteristic frequency should be approximately 10-15 Hz higher. These cavities have also multi-port flow exits and they are angled with respect to the main flow direction. Part of the pressure wave reaching the flow exists is then reflected back. It lowers the pressure near the semilunar valves (P, A) causing the backflow. Also ventricular relaxation takes place and adds additional suction. This, in turn, leads to these valves closure. When the valves are closed, the pressure wave reflects back from the valve's membrane. This reflection is responsible for two major sound peaks $S2_3$ and $S2_5$ shown in Fig. 3a. $S2_3$ peak is due to the reflection from the aortic valve membrane, while $S2_5$ is due to the reflection from the pulmonary valve membrane. Small amplitude high frequency peaks preceding $S2_3$ and $S2_5$ may indicate that the pressure wave first reflects from the walls of pulmonary and aortic cavities located on the opposite sides from the semilunar valves. According to the frequency spectrum shown in Fig. 3b, they have frequency peak at 115 Hz. This suggests that characteristic dimension of the pulmonary and aortic cavities may be close to 0.9 cm. We speculate that all pressure spikes on S1 and S2 have functional mechanical explanation and are not caused by *self-sustained* flow instabilities or so-called 'turbulence'. In the future work, we will extend our model to understand complex fluid–related nature of the heart murmurs. We will also attempt to link them with the mechanical heart dysfunctions.

SCOPE OF CFD ANALYSIS

CFD analysis can help us to verify the above assumption. We can simulate the generic incompressible start-up flow condition (that mimics the ejection event in the cardiac cycle) and monitor pressure changes in the specific points inside the computational domain (see Fig. 9b). We begin by studying generic simplified cases (see Fig. 7). Later, we will expand the scope into the three-dimensional moving boundaries fluid structure interaction problems. At first we studied flow in the obstructed vessel (Fig.6) using commercial fluid mechanics software code CFD-ACE+ [15]. Both constant and non-Newtonian blood flow viscosity models were employed. We used channel with characteristic dimension of 1 cm and velocities in the range of several meters per second were considered. Our objective was to calculate transient fluid flow (start from the rest, u=v=0) and to monitor pressure fluctuations in time. Dynamic flow transition and recirculation structures are clearly evidenced from the Figure 6. But flow had quickly stabilized and we found no significant flow induced pressure fluctuations. We then introduced time tabulated sharp flow velocity pulse. Pressures were measured at several positions behind the last restriction. They had accurately followed the shape of the specified boundary condition (velocity pulse) and they had not generated any derived pressure pulsations or frequencies.

This limited study confirmed that it is not possible to create pressure oscillations in a small diameter channel with the direct blood flow. This was true even when the cross-section was very restricted. Typical Re numbers are shown in Table 4 and expected to be in excess of 1000. We will also need to study pulsating flow conditions with the negative velocity (backflow). It is possible to create pressure oscillations due to the flow instabilities (and vortex formations) in some other blocked flow configurations at higher Reynolds numbers, see the results presented in Figs. 8(a,b), Fig. 9 and Fig. 10. These results were obtained in our previous studies [9-11]. In Fig. 8a we show transient oscillatory flow formations for three characteristic times between t=0..2 (non-dimensional time, for the square channel of non-dimensional length=1). As we can see, the high frequency pulsations arise due to the transient vortical flow structures. The inlet velocity was maintained at non-dimensional velocity U=1. This simulation was performed for Re=10,000. Typical Re numbers for blood heart vessels start at 300 [12] and for the heart chambers are between 7,000 to 11,000 [13,14], see also Table 4.

Our next analysis was focused on a transient flows (from the start) developing in a similar "blocked" geometry. Our results for Re=1000 are shown in Fig. 9a. We can see that pressure spikes can develop when strong inlet flow fills the volume occupied with the fluid at rest. Results shown in Fig. 9a [9,10] demonstrate several damped oscillatory pressure spikes that happen prior to final pressure settlement. Our results obtained using CFD-ACE+ [15] are demonstrated in Figs. 9b and 11(a,b,c,d). They indicate that in all considered cases pressure fluctuation (due to incoming velocity) is self-stabilizing. Pressure rises very quickly (order of 1 ms) and then drops quickly down in 10 to 30 ms (see Fig. 9b). We will continue our studies considering stronger blockages and higher velocities thus trying to establish transient flow formations similar to those shown in Fig. 10 (Re=1250, [9]). It is anticipated that for the normal human heart operation such conditions may be rare. This would explain why we do not see significant secondary peaks in S1 and S2, and that serious heart valvular or other malfunctions will be required to generate strong flow vortices and pressure pulsations.

FUTURE WORK

In our future work we will generate prototype ventricle, pulmonary, aorta and atrium shapes to study in 2D possible pressure oscillations due to the transient flow conditions.

These conditions include:

a) flow starting from the rest;
b) pulsatile flow with the backflow zones;
c) flow startup with initially blocked exit and with subsequently blocked inlet;
d) start of the flow with partially blocked exit with subsequently blocked inlet.

These conditions directly correspond to various events in the cardiac cycle (#1-14) described in Figure 5. We will run transient flow problem with the specified explicit sequence of events. They will include fluid at rest, the inlet flow pulse (injection), inlet closure (valve closure), transient flow settlement in the enclosed volume and finally exit opening (simulating semilunar valve opening) and flow ejection out of the chamber.
We will also simulate another problem mimicking the aortic and pulmonary areas. In this case right inlet (valve) will be replaced by the wall and left exit will be partially restricted. This should allow us to study flow reflection and other peculiarities of the S2 sound.

Figure 1. Digital Auscultation Equipment

CONCLUSIONS

The presented analysis has showed that it is highly unlikely that S1 and S2 sound pressure spikes occur due to the blood inflow into the pulmonary and aortic areas or due to the flow turbulence. This contradicts to some widely accepted assertions [5]-[7]. Certain flow boundary conditions may lead to the small amplitude high frequency pressure fluctuations known as heart murmurs which can appear during the systole (between S1 and S2) and diastole. CFD results shown on Figs. 8b, 9a and 10 confirm this possibility. Heart Sounds are considered to be multi-component. Our initial observations demonstrate that normal heart sounds may contain a non-overlapping combination of several single components.

REFERENCES

[1]. Reed T.R., Reed N.E., Fritzson P., "The Analysis of Heart Sounds for Symptom Detection and Machine-Aided Diagnosis", Proceedings of the 4th International EUROSIM Congress and the 2nd Conference on Modelling and Simulation in Biology, Medicine and Biomedical Engineering, Deft, Netherlands, June 26-29, pp. 1-6, 2001.
[2]. Xu J., Durand L.G., Pibarot P., "Nonlinear Transient Chirp Modeling of the Aortic and Pulmonary Components of the Second Heart Sound", IEEE Transactions on Biomedical Engineering, Vol. 47, No. 7, pp. 1328-1334, July 2000.
[3]. Durand L.G., Pibarot P., "Digital signal processing of the phonocardiogram: Review of the most recent advances", CRC Critical Reviews in Biomedical Engineering, vol. 23, pp. 163-219, 1995.
[4]. Rangayyan R.J., Lehner R.J., "Phonocardiogram signal analysis: a review", Durand L.G., Pibarot P., "Digital signal processing of the phonocardiogram: Review of the most recent advances", CRC Critical Reviews in Biomedical Engineering, vol. 15, pp. 211-236, 1988.
[5]. Lehrer S., "Understanding Pediatric Heart Sounds", Saunders, New York, 2003.
[6] "Auscultation Skills: Breath & Heart Sounds", Springhouse, Pennsylvania, 1998.
[7]. Rushmer D., "Cardiovascular Dynamics", Sounders, Philadephia, 1976
[8]. BSignal- Phonocardiograph, http://www.bsignetics.com
[9]. V.V. Kudriavtsev, M.J. Braun, "Model Developments for the Brush Seal Numerical Simulation", Journal of Propulsion and Power", Vol. 12, No. 1, Jan-Feb, 1996, pp. 193-201
[10]. V.V. Kudriavtsev, "Numerical Analysis of the Transient Fluid Flows in the Brush Seal Elements for Aerospace Industry", Ph.D. Dissertation, 1993, Moscow Aviation Institute, pp. 1-206 (in Russian)
[11]. V.V. Kudriavtsev, M.J. Braun, "Fluid Flow Structures in Staggered Banks of Cylinders Located in a Channel", ASME Journal of Fluids Engineering, Vol. 117, March 1995, pp. 36-44
[12]. K. Onogi, K. Kohge, K. Minemura, "Numerical Simulation of Blood Flow Through Stenosed Vessel", Proceedings of the ASME/JSME 5th Int. Symp. On Computational Technologies for Fluid/Thermal/ Chemical/Stressed Systems with Industrial Applications ,PVP 2004, July 25-29, San Diego La Jolla, pp. 1-10
[13]. A. Qiao, T. Matsuzawa, "Hemodynamics of End-to-end Femoral Bypass Graft", Proceedings of the ASME/JSME 5th Int. Symp. On Computational Technologies for Fluid/Thermal/Chemical/Stressed Systems with Industrial Applications, PVP 2004, July 25-29, San Diego La Jolla, pp. 1-10
[14]. M. Watanabe, T. Matsuzawa, "Computational Simulation of Flow in a Dissecting Aortic Aneurism Reconstructed from CT Images", Proceedings of the ASME/JSME 5th Int. Symp. On Computational Technologies for Fluid/Thermal/Chemical/ Stressed Systems with Industrial Applications ,PVP 2004, July 25-29, San Diego La Jolla, pp. 1-6
[15]. CFD-ACE+ V2003, http://www.cfdrc.com

Table 1. **Heart Sound Timing during Single Beat (Fig. 4a)**

S1 Begins, sec	S1 ends, sec	S2 begins, sec	S2 ends, sec
0.092	0.225	0.507	0.587

Table 2. **S1 Heart Sound Timing during Single Beat (Fig. 2a)**

First Peak	Second Peak	Third Peak, sec	Fourth Peak, sec	Fifth Peak, sec
0.118	0.150	0.176	0.203	0.215

Table 3. **S2 Heart Sound Timing during Single Beat (Fig. 3a)**

First Peak, sec	Second Peak, sec	Third Peak, sec	Fourth Peak, sec
0.158	0.173	0.198	0.215

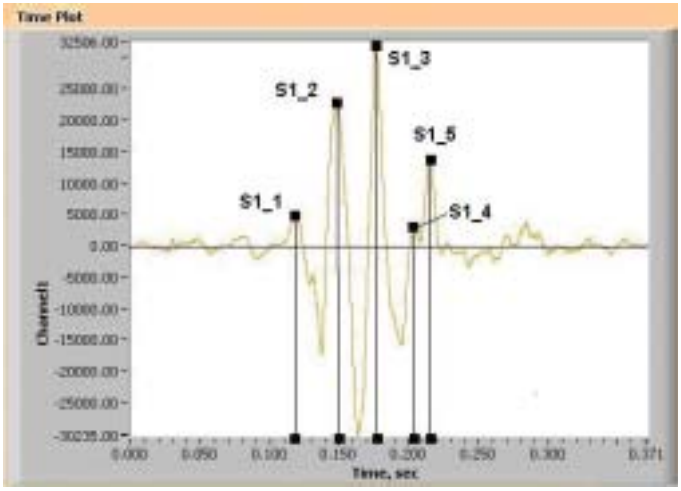

Figure 2a. S1 Heart Sound Shape and Timing

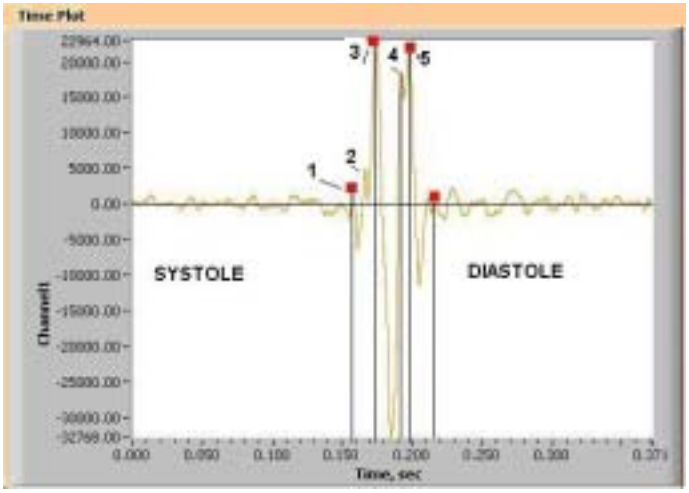

Figure 3a. S2 Heart Sound Shape and Timing

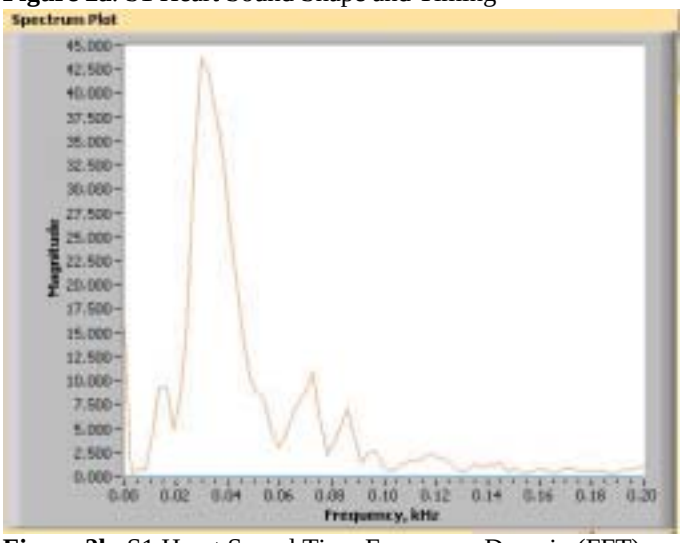

Figure 2b. S1 Heart Sound Time Frequency Domain (FFT)

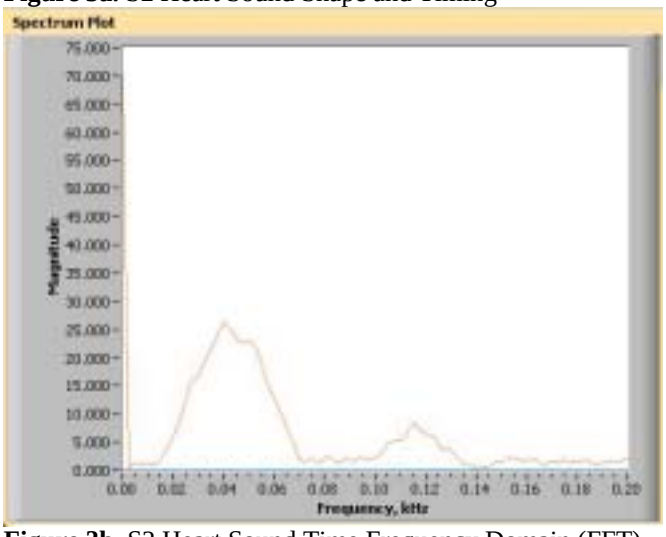

Figure 3b. S2 Heart Sound Time Frequency Domain (FFT)

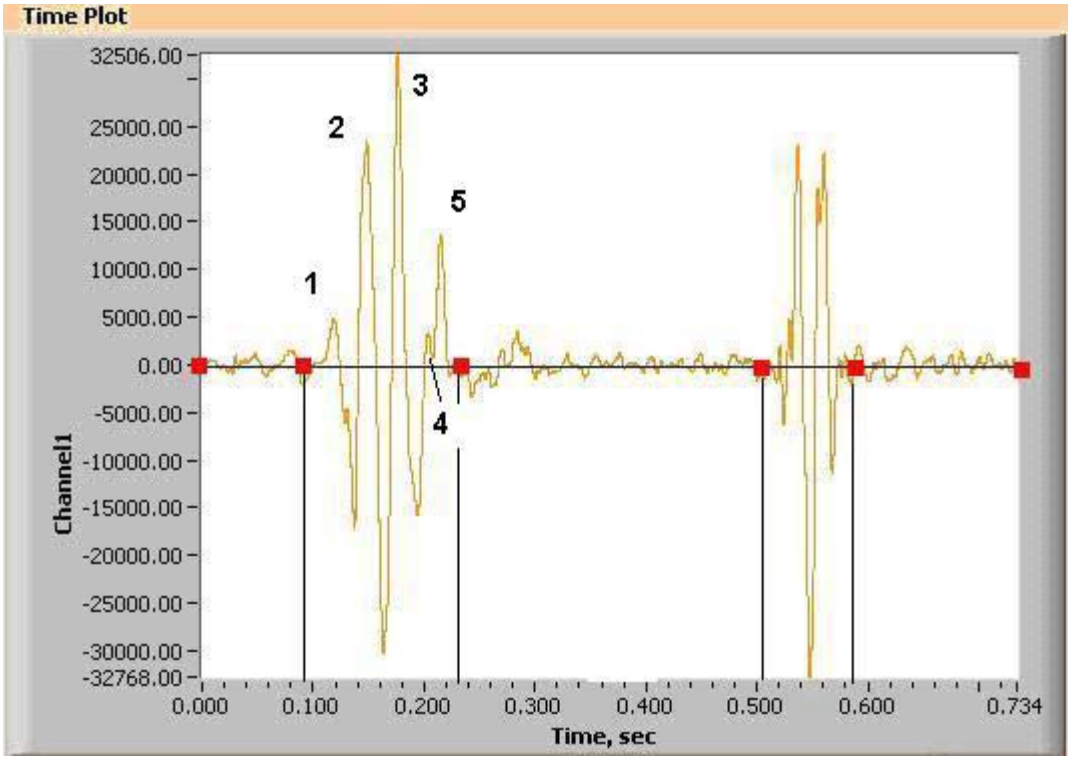

Figure 4a. Normal Heart Sound (single beat) showing S1 and S2 components.
Data is collected by the authors using Cardionics Corp Electronic Stethoscope and Windows Recorder

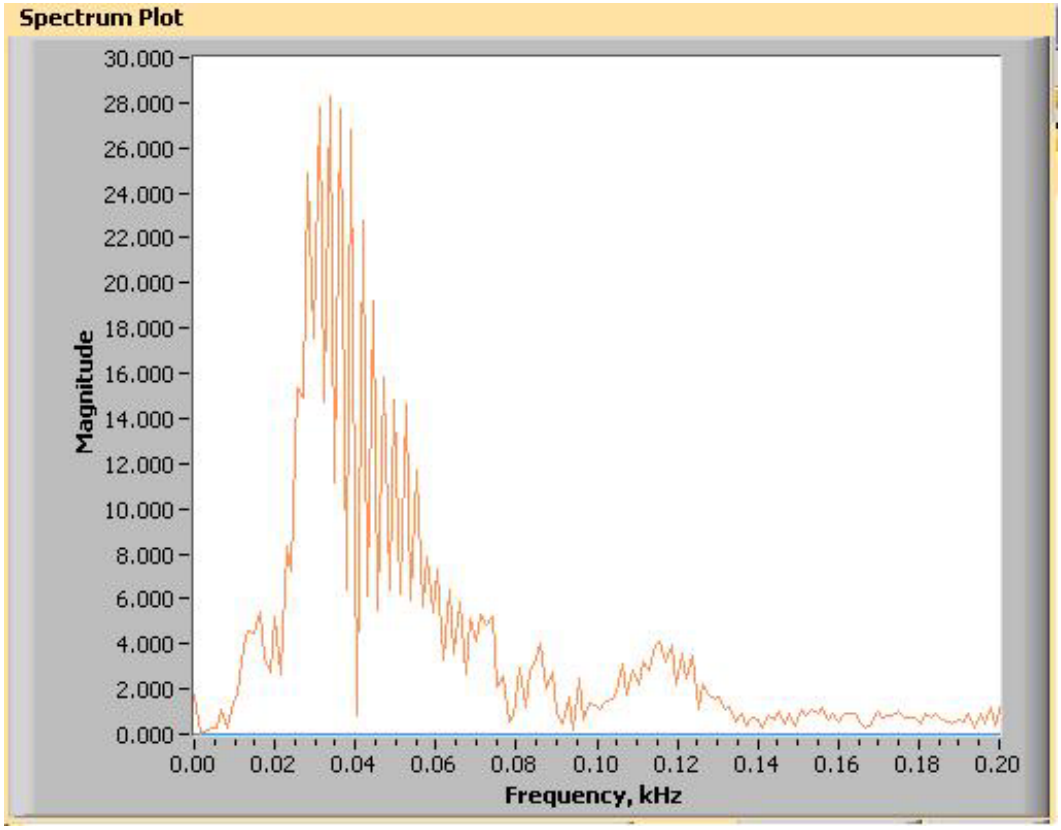

Figure 4b. Normal Heart Sound (single bit) corresponding time domain frequency distribution.
Data is processed using BSignal Phonocardiograph from BioSignetics Corp.

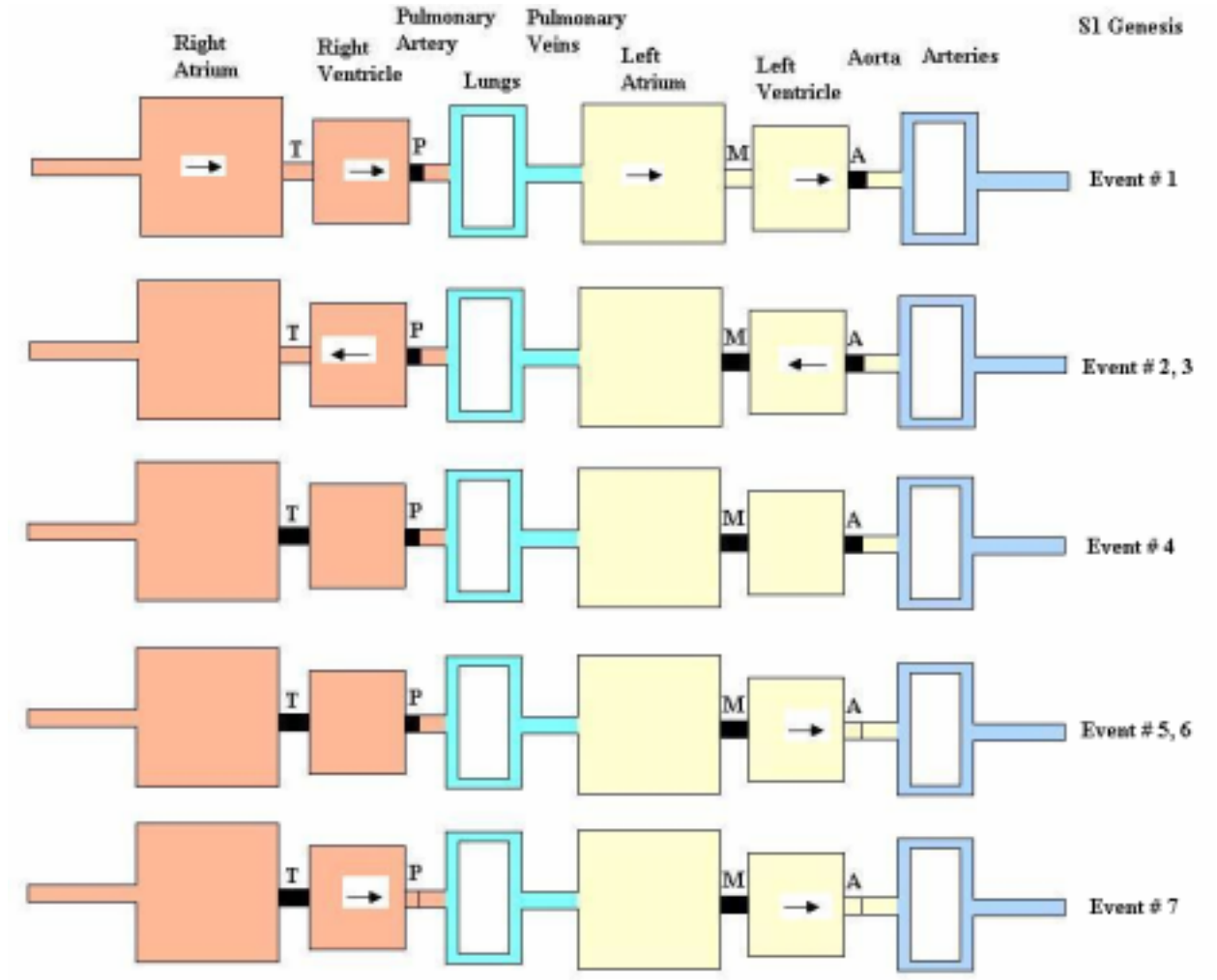

					T	P	M	A
Event #	Duration, ms	Cardiac Cycle	Period Name	Heart Sound	Tricuspid	Pulmonic	Mitral	Aortic
1		Systole	Ventricular Systole		Opened	Closed	Opened	Closed
2		Systole	Ventricular Systole	Start S1	Opened	Closed	Closes	Closed
3		Systole	Ventricular Systole		Closes	Closed	Closed	Closed
4	20-30	Systole	Isovolumic Contraction	S1 - max amplitude	Closed	Closed	Closed	Closed
5		Systole	Ejection		Closed	Closed	Closed	Opens
6		Systole	Ejection		Closed	Opens	Closed	Opened
7		Systole			Closed	Opened	Closed	Opened
8		Diastole	Isovolumic Relaxation	Start S2	Closed	Opened	Closed	Closes
9		Diastole	Isovolumic Relaxation		Closed	Closes	Closed	Closed
10	30-60	Diastole	Isovolumic Relaxation	End of S2	Closed	Closed	Closed	Closed
11		Diastole			Opens	Closed	Opens	Closed
12		Diastole	Rapid Inflow		Opened	Closed	Opened	Closed
13		Diastole	Diastasis		Opened	Closed	Opened	Closed
14		Diastole	Atrial Systole		Opened	Closed	Opened	Closed

Figure 5. Mechanical Schematics of Heart Chambers and Valves Operations

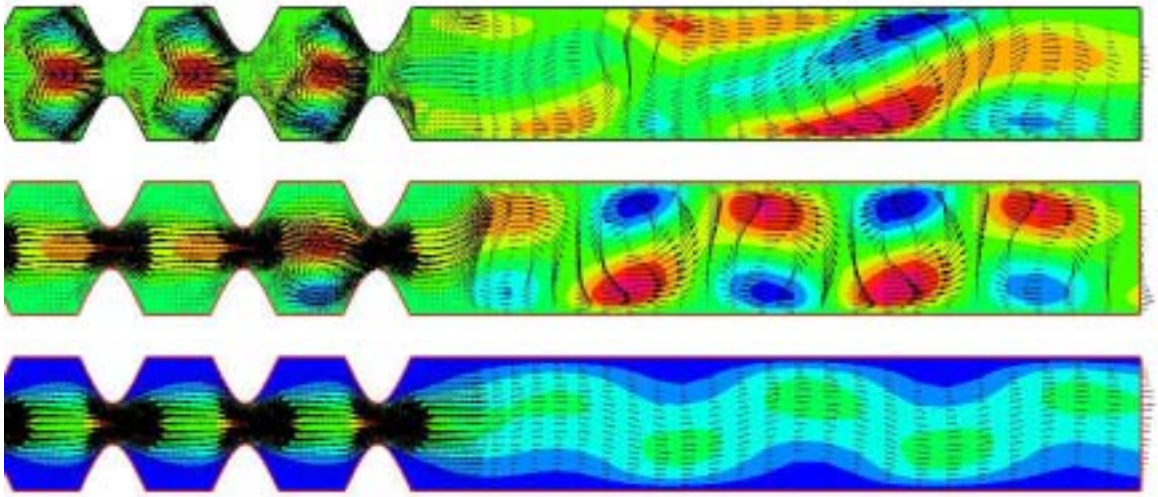

Figure 6. CFD illustrations of the flow fluctuations past the sudden contraction for transient flow

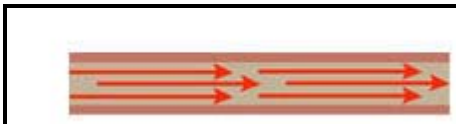

a) Increased through flow, anemic case

b) Stenosis causes obstruction to flow

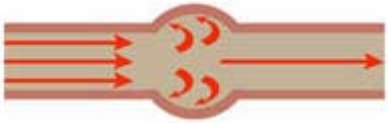

c) Flow into a dilated chamber (aorta)

d) Vibrating membrane–pupillary muscle rupture

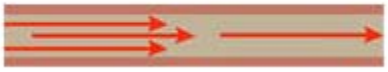

e) Leakage flow, ventricular septal defect

Figure 7. Fluid Mechanics Causes of Heart Diseases (from Murmur Wizard)

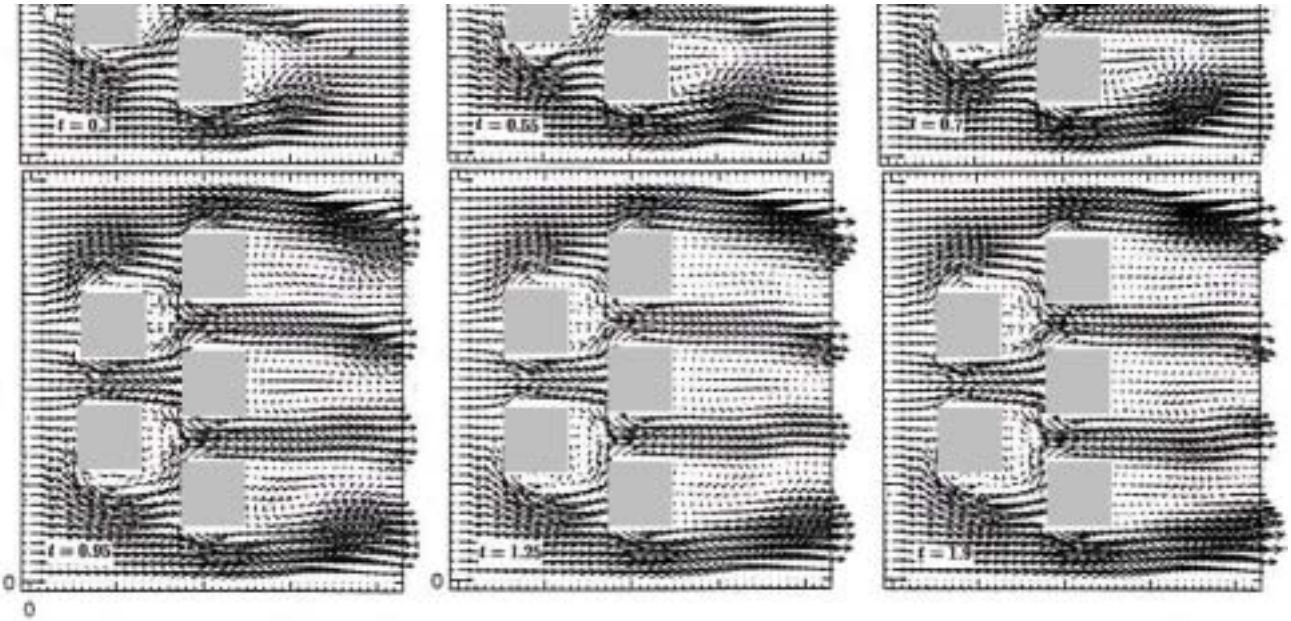

Figure 8a. Transient Flow in the Blocked Square Channel (t=0.95;1.25;1.9), Re=10,000

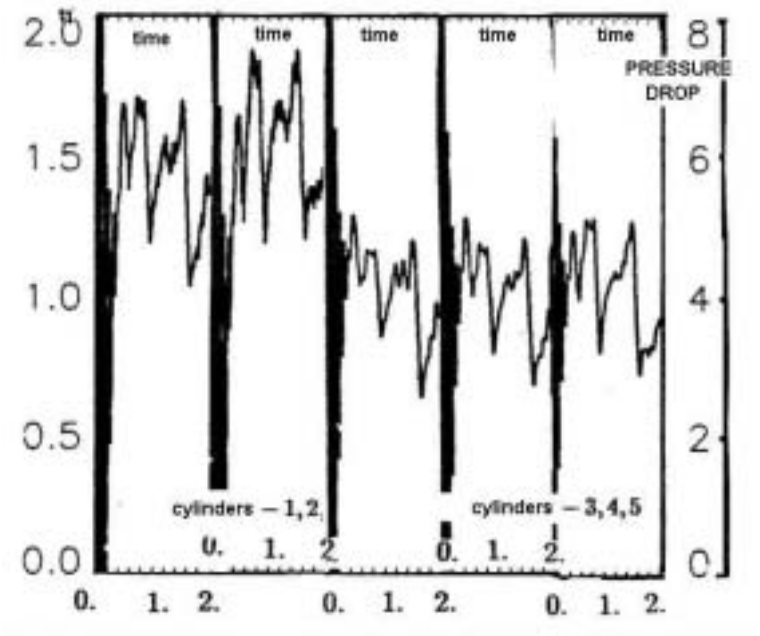

Figure 8b. Matching Pressure Drop Oscillations, Re=10,000

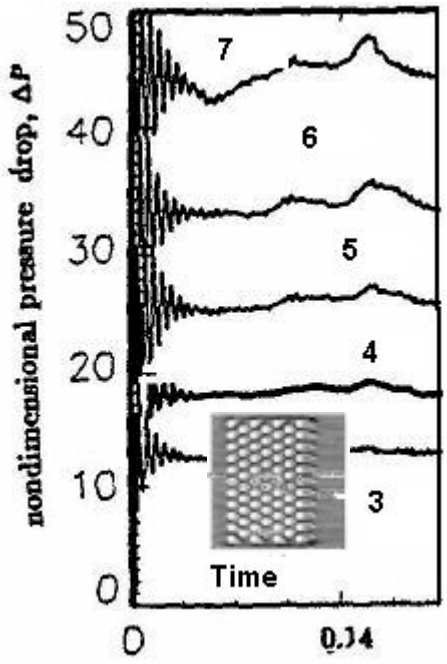

Figure 9a. Transient Pressure Drop showing oscillatory start from rest (u=v=0), Re=1000

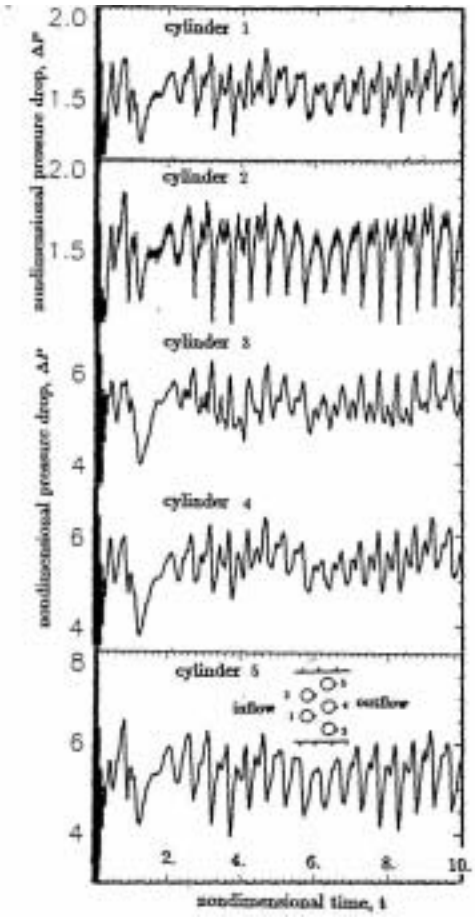

Figure 10. Pressure Oscillations in a restricted Channel, Re=1250

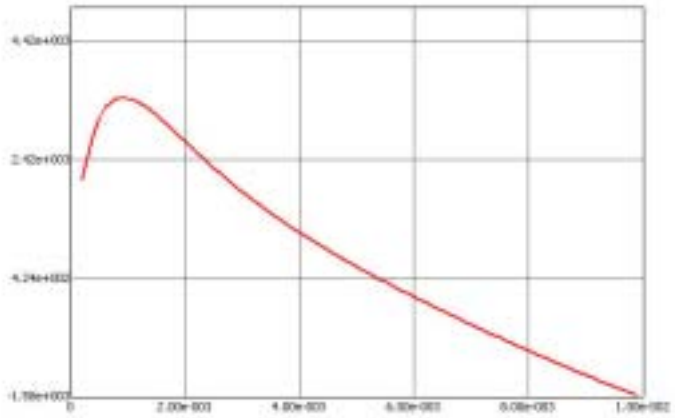

Figure 9b. Pressure history behind the second row of cylinders. Pressure rise at the flow onset and quickly stabilizes (delta*t*=0.01 sec =10 ms, inlet velocity=1 m/s, vertical height=4 cm). Vertical axis –Pressure (Pa) and horizontal axis –Time (s).

Table 4. Reynolds Number Estimations

Velocity	Visc.	Density	Length	Re_l
0.1	8.55E-04	997	0.01	1.17E+03
0.25	8.55E-04	997	0.01	2.92E+03
0.5	8.55E-04	997	0.01	5.83E+03
1.2	8.55E-04	997	0.01	1.40E+04

Water Flow Model

Velocity	Visc.	Density	Length	Re_l
0.1	3.50E-03	997	0.01	2.85E+02
0.25	3.50E-03	997	0.01	7.12E+02
0.5	3.50E-03	997	0.01	1.42E+03
1.2	3.50E-03	997	0.01	3.42E+03

Classon's Blood Viscosity Model

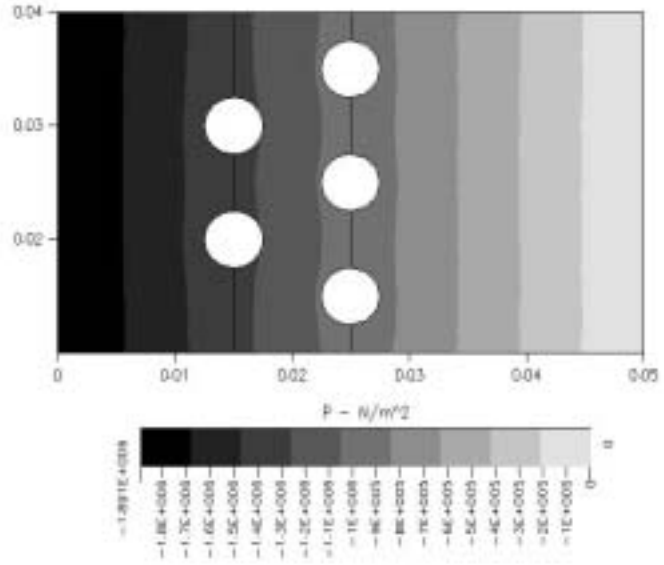

Figure 11a. Transient Flow Development, time =0.1 ms At t=0 u=v=0; at t>0 u=1. Inlet pressure is high (1.89E6Pa)

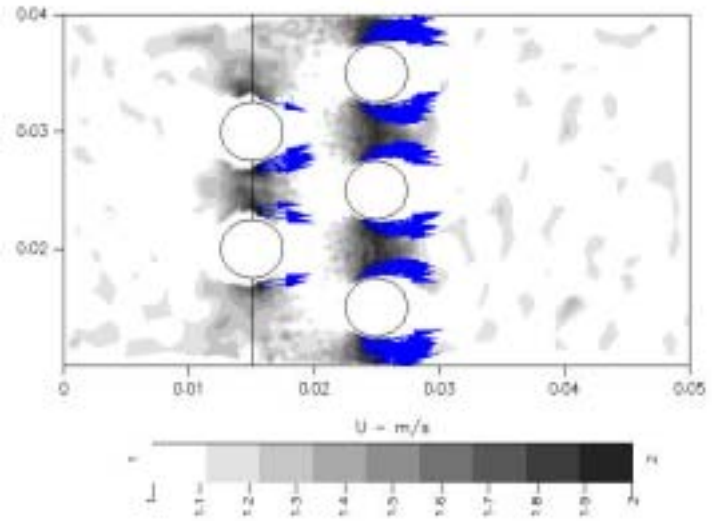

Figure 11b. Transient Flow Development, time =0.1 ms Horizontal velocity distribution.

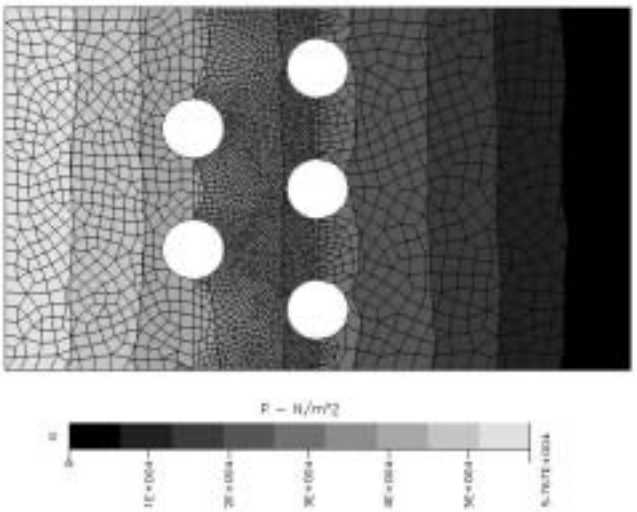

Figure 11c. Transient Flow Development, time =1 ms. Inlet pressure is low (6.76E4 Pa)

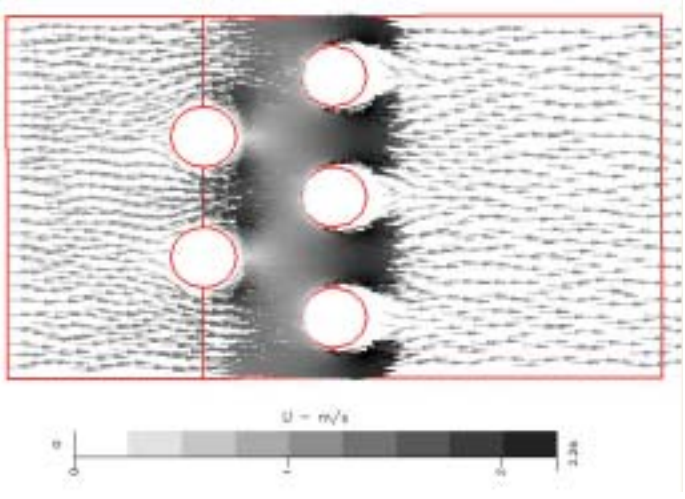

Figure 11d. Transient Flow Development, time =1 ms.